



Adsorption and recovery of U(VI) from actual acid radioactive wastewater with low uranium concentration using thioacetamide modified activated carbon from liquorice residue

Yan Tan^{1,2,3} · Le Li^{2,3} · Hui Zhang² · Dexin Ding^{1,2} · Zhongran Dai² · Jinhua Xue^{2,3} · Jinquan Liu^{2,3} · Nan Hu² · Yongdong Wang²

Received: 14 March 2018 / Published online: 22 June 2018

© Akadémiai Kiadó, Budapest, Hungary 2018

Abstract

In this paper, cheap liquorice residue was used to prepare activated carbon (AC), thioacetamide (TAA) was used to modify the AC, and the adsorption experiments were conducted in the simulated acid radioactive wastewater with low uranium concentration to study the adsorption behavior and mechanism for uranium by TAA modified AC (TAA-AC). The removal efficiency by TAA-AC was 92.1–98.2% from the 1 mg L⁻¹ uranium solution at pH 2–6. The adsorption equilibrium data were well fitted by Dubinin–Radushkevich model, and the maximum adsorption capacity was estimated to be 340 mg g⁻¹. TAA-AC showed an enhanced selectivity for uranium in the presence of competitive ions. Furthermore, the adsorption experiments were conducted in the actual acid radioactive wastewater with low uranium concentration from an in situ leach uranium mine. The high adsorption rate (98.3%) and selectivity ($K_d = 3.78 \times 10^4$ mL g⁻¹) for uranium were observed in the actual acid radioactive wastewater, and the adsorption rate was found to maintain 96.2% over six cycles of adsorption–desorption.

Keywords Liquorice residue · Thioacetamide · Activated carbon · Uranium · Actual acid radioactive wastewater

Introduction

Uranium mining and processing generate huge amounts of radioactive wastewater with uranium concentration lower than 1.0 mg L⁻¹ [1]. Because the uranium in the wastewater has chemical toxicity, radioactivity and long half life,

it is a long term threat to human beings and the environment if not treated effectively [2–5]. Therefore, many investigators around the world have paid much attention to the treatment of the wastewater [6–10]. So far, many methods have been proposed, and adsorption has been found to be a simple, effective and economic one with high potential for the removal and recovery of uranium from the neutral or near neutral radioactive wastewater [11–17].

However, uranium is extracted from ore by acid process in China, and the produced large volume of radioactive wastewater with low uranium concentration is acidic [18–20]. Furthermore, the uranium in the acid wastewater is easy to migrate into the environment, and it will cause significant pollution to the environment if the wastewater is not treated effectively [21]. Therefore, it is necessary to develop adsorbents for treating the acid radioactive wastewater with low uranium concentration.

Although many adsorbents such as Amberlite IRA-402 resin [22], trioctylamine impregnated polyurethane foam [23], PVC cement [24] and commercial activated carbon [25] have been developed for the adsorption of uranium from acid solution, they were only suitable for the

Electronic supplementary material The online version of this article (<https://doi.org/10.1007/s10967-018-5952-8>) contains supplementary material, which is available to authorized users.

✉ Dexin Ding
dingdxzz@163.com

¹ School of Resources and Safety Engineering, Central South University, Changsha 410083, China

² Key Discipline Laboratory for National Defense for Biotechnology in Uranium Mining and Hydrometallurgy, University of South China, Hengyang 421001, China

³ School of Public Health, University of South China, Hengyang 421001, China

treatment of acid radioactive wastewater with high uranium concentration, not suitable for the treatment of the acid radioactive wastewater with low uranium concentration. In addition, the acid radioactive wastewater with low uranium concentration is complicated in composition. These characteristics make its treatment more difficult.

The activated carbon (AC) is considered to be an ideal adsorbent for uranium in radioactive wastewater due to its unique pore structure, large specific surface area, and structural stability in acid solution [26–31]. But it is important to get a cheap source material to prepare it, because the AC obtained from non-recycled materials such as coal and farm produce is expensive [32]. Liquorice is a commonly used Chinese traditional medicinal herb, and its residue discarded by Chinese drug companies is up to tens of thousands of tons annually. Liquorice residue is a cheap source material for the preparation of activated carbon because it is abundant in lignin, high in carbon content, low in cost and not easy to rot after drying [33, 34].

In order to improve the adsorption capability and selectivity of AC for uranium in acid solution with low uranium concentration, its surface should be modified to have as many as possible groups which can bind U(VI) ions. The thioacetamide (TAA) has many such groups including C=S and N–H groups, and it can be used to modify AC by condensation reaction with formaldehyde. This chemical modification can make these groups firmly adhere on the surface of AC and the adsorbent will remain stable in acid radioactive solution. Moreover, the modification process is simple under mild conditions and is easy to be operated, therefore, it has potential for application.

In this work, liquorice residue was used to prepare AC, and TAA was used to modify AC. The TAA modified AC (TAA–AC) was used to conduct the adsorption experiments in the acid radioactive wastewater. The effects of pH, contact time, adsorbent dose, initial uranium concentration and temperature were investigated. The morphology and adsorption properties of TAA–AC were characterized by scanning electron microscope (SEM), energy dispersive X-ray analysis (EDX), Fourier transform infrared spectroscopy (FTIR), X-ray Photoelectron spectroscopy (XPS), X-ray diffraction (XRD), zeta potential and point of zero charge (pH_{pzc}), and the isotherm, kinetic and thermodynamic characteristics were determined. Furthermore, the adsorption experiments were conducted on the actual acid radioactive wastewater from an in situ leach uranium mine, and selectivity and adsorption–desorption cycling property were also investigated. The objective of this study is to develop an effective and economic adsorbent for removal and recovery of uranium from the actual acid radioactive wastewater with low uranium concentration from an in situ leach uranium mine.

Experimental

Reagents

All of the chemical reagents used were analytical grade. The ultrapure water was used in all experiments. TAA was purchased from Kermel Chemical Reagents Development Center (Tianjin, China). Zinc chloride and formaldehyde were purchased from Damao Chemical Reagent Factory (Tianjin, China).

The uranium stock solution was prepared by referring to the articles [35, 36]. The different concentrations of stock solutions were kept in acidic condition, and the uranium solutions were prepared by diluting the stock solution to appropriate volumes immediately before experiments. Na_2CO_3 or HCl solutions were used to adjust pH.

Preparation of AC from liquorice residue

Liquorice residue was obtained from liquorice slices (Ning-Xia, China) after being decocted with water, washed several times with ultrapure water and dried at 333 K for 48 h. Liquorice slices were crushed and passed through a 100 mesh sieve.

Licorice powder was immersed in 50% (w/w) zinc chloride, and the mixture was heated and stirred until the paste was obtained. Then, the produced paste was placed in a drying oven at 338 K for 10–14 h to get rid of moisture and activated in microwave oven with 640 W for 10 min. Finally, the obtained activated carbon (AC) was washed and filtered with large amount of ultrapure water, and then dried at 368 K for 48 h.

Preparation of TAA–AC

The prepared AC was suspended in 4 mol L^{-1} nitric acid solution, and the solution was heated and stirred at 333 K for 2 h. This made its surface contain more oxygen groups [37]. 2.5 g thioacetamide was dissolved in 25 mL ultrapure water and 6 mL methanol by heating and stirring. 5 g AC was added into the solution, and the mixture was ultrasonicated for 3 h and then stirred with a magnetic stirrer. Subsequently, 1 mL acetic acid and 15 mL 30% (w/w) formaldehyde were added into the mixture drop by drop. After that, the mixture was stirred and refluxed at 343 K for 3 h and at normal temperature for 2 h. Finally, it was filtered, washed with ultrapure water and ethanol for several times, dried at 313 K, and the TAA–AC was obtained. The synthesis route for preparing TAA–AC was shown in Fig. 1.

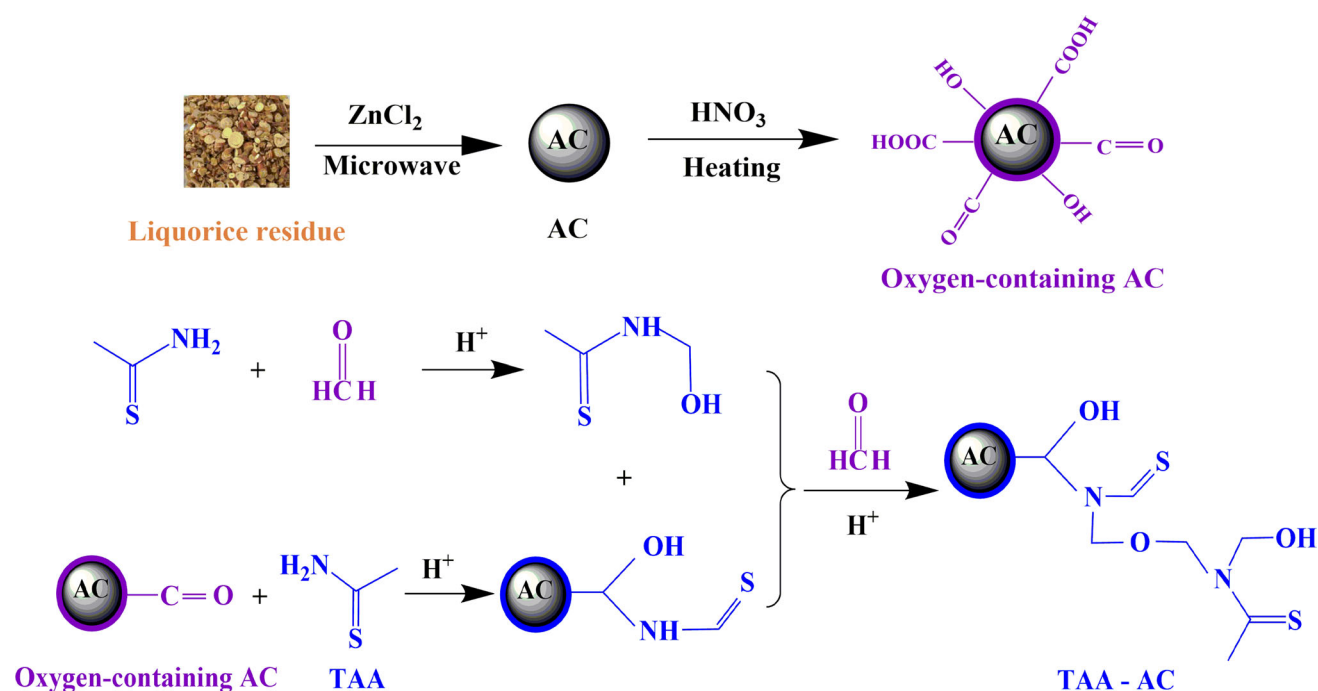


Fig. 1 Synthesis route for preparing TAA-AC

Adsorption experiments on simulated acid radioactive wastewater

Batch adsorption tests were performed in a reciprocating thermostated air bath shaker. 100 mL solution with uranium concentration of 1 mg L^{-1} was mixed with 160 mg TAA-AC in 250 mL Erlenmeyer flask, and it was shaken at 200 rpm for 2 h at 308 K. The upper solution was centrifuged at 10,000 rpm for 10 min after adsorption, and the concentrations of uranium in supernatant were analyzed by trace uranium analyzer (WGJ-III, China). The relative standard deviation for 7 samples with uranium concentration of $5 \mu\text{g L}^{-1}$ was 3.9% and the recovery was 95.5–104.3%. Each test was repeated thrice and the average values were obtained. Blank samples without TAA-AC served as control.

The removal efficiency $R\%$, the adsorption capacity of the adsorbent Q (mg g^{-1}), and the distribution coefficient K_d (mL g^{-1}) were calculated from the following equations, respectively:

$$R\% = \frac{100(C_0 - C_e)}{C_0} \quad (1)$$

$$Q = \frac{(C_0 - C_e)V}{1000M} \quad (2)$$

$$K_d = \frac{(C_0 - C_e)V}{C_e M} \quad (3)$$

where C_0 (mg L^{-1}) and C_e (mg L^{-1}) are the initial and final concentrations of U(VI) ions, respectively, V (mL) is the

volume of solution; and M (g) is the dry weight of adsorbent.

Adsorption experiments on actual acid radioactive wastewater

The actual acid radioactive wastewater was taken from an in situ leach uranium mine in Northwest China. Adsorption tests of U(VI) by the TAA-AC were conducted in conical asks (250 mL) to determine its adsorption capability. 0.16 g TAA-AC was added to 100 mL acid wastewater containing uranium, and the mixtures were then shaken on a rotary shaker at 200 rpm and 308 K for 10 h. The changes of uranium concentration were measured in different contact times.

Desorption and regeneration experiment

In order to regenerate the TAA-AC loaded with U(VI), desorption test was carried out using 0.5 mol L^{-1} HCl, 0.5 mol L^{-1} HNO₃, 0.25 mol L^{-1} H₂SO₄ and 0.5 mol L^{-1} EDTA. The U(VI) loaded TAA-AC was dispersed in different desorption agent and shaken on air bath oscillator for 6 h. Then, the mixture was centrifuged at 5000 rpm for 40 min. After that, The concentration of U(VI) in eluent was determined. The adsorbent was collected, washed with ultrapure water, dried and reused for adsorption test, and the adsorption-desorption process was repeated six times.

Characterization

Fourier transform infrared spectra (FTIR) were measured using a Nicolet 380 FT-IR spectrometer (USA). Scanning electron microscope (SEM) images were obtained for the adsorbent before or after adsorption of uranium using a JSM-6360LV microscope (Japan). Energy Dispersive Spectrometer (EDS) was detected using EDX-GENESIS60S (USA) for the transformation of chemical element during the adsorption process. The qualitative X-ray powder diffractometry (XRD) for main crystalline compounds of the adsorbent samples were identified by using a Bruker D8 advance (Germany). X-ray photoelectron spectroscopy (XPS) was measured in a Thermo Fisher ESCALAB 250Xi by using an aluminum anode ($Al K_{\alpha} = 1486.6$ eV radiation). The pH_{pzc} was measured by a PB-21 pH meter (Germany). The zeta potential was measured by a Zetasizer NanoZS (Malvern, UK).

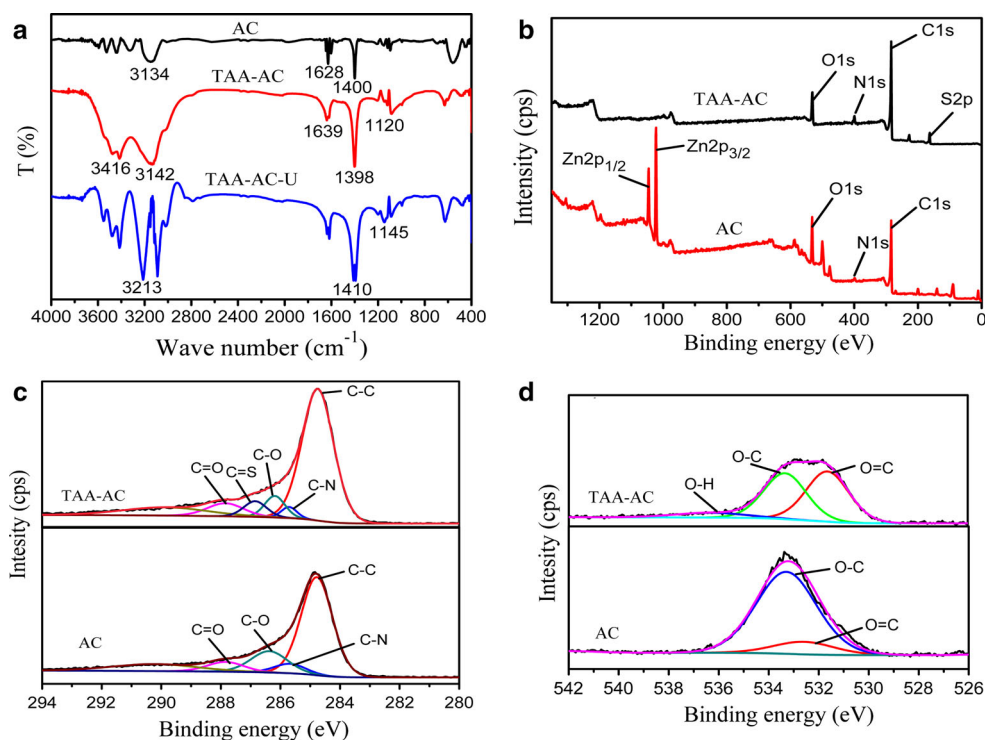
Results and discussion

Material characterization

The FT-IR spectra of the AC and TAA-AC was shown in Fig. 2a. In the spectrum of AC, the peak at 1400 cm^{-1} was from the C-H bending vibration, and the peak at 3134 cm^{-1} was assigned to the stretching vibration of hydroxyl groups of the adsorbed water. The spectrum of

TAA-AC showed that the peak at 3134 cm^{-1} shifted to 3142 cm^{-1} . The peak at 3416 and 1639 cm^{-1} arose from the stretching and bending vibration of N-H. A new peak was observed at 1120 cm^{-1} which might belong to the stretching vibration of C=S, and this demonstrated that TAA had been impregnated into AC after preparation. Figure 2b showed the XPS spectra of AC and TAA-AC. By comparing the survey spectra, it was found that a new peak of S2p appeared and the intensity of N1s-peak greatly enhanced in the spectrum of TAA-AC (Elemental composition determined by X-ray photoelectron spectroscopy as shown in Table S1), which indicated the addition of the sulfur and nitrogen elements on TAA-AC surface. There were two peaks of Zn2p_{1/2} and Zn2p_{3/2} in XPS spectrum of AC, which were produced in AC preparation. However, no zinc peaks were found in XPS spectrum of TAA-AC. This indicates that the zinc ions were completely eluted in the subsequent preparation process, and they would not affect the experiment results. The C1s spectra of the AC and TAA-AC were shown in Fig. 2c. The peaks of C-O, C=O and C-N was found on the surface of AC and TAA-AC, the peak of C-N shifted from 258.59 eV on AC to 285.89 eV on TAA-AC, and a new peak of C=S appeared in the spectrum of TAA-AC. As shown in Fig. 2d, the peak of C=O and C-O was observed in the O1s spectrum of the AC, the peak of C=O shifted from 532.56 eV on AC to 531.68 eV on TAA-AC, and its intensity became stronger. In addition, a new peak of hydroxyl appeared in the spectrum of the TAA-AC. The results further

Fig. 2 a FT-IR spectra of AC, TAA-AC, and TAA-AC-U, b XPS spectra of AC and TAA-AC, c XPS spectra of C1s, and d O1s for AC and TAA-AC



demonstrated the structure of the synthesized TAA–AC (Fig. 1). The C=S and amino group was widely recognized as an effective active site for the adsorption of U(VI) ions. Moreover, hydroxyl group could also coordinate with U(VI) ions through electrostatic interaction and hydrogen bond.

The microstructures of AC and TAA–AC were characterized by SEM, as shown in Fig. 3. The original AC had a porous and loose surface structure (Fig. 3a), which indicated that the AC had large specific surface area which could provide the abundant channel and sufficient space. Figure 3b showed that the surface of TAA–AC was rough and bright, which suggested that AC was bonded with TAA. The zeta potentials of the AC and TAA–AC were measured in water, as shown in Fig. S1. The surface of AC had a slight positive charge (3.00 mV), while the TAA–AC possessed a negative zeta potential value (-4.40 mV). These results further validated that the TAA modified reaction on the surface of AC was successful.

The EDX spectra of TAA–AC loaded with uranium was shown in Fig. 4a, the peak of uranium was clearly observed. From the elemental analysis as showed in Fig. 4a inset, it can be found that the weight percentage of U(VI) adsorbed on the TAA–AC amounted to 3.76%. This indicated that the TAA–AC could adsorb U(VI) efficiently. As showed in Fig. 4b, the XPS spectra of U4f attributed to U(VI) could be resolved into the peak of U4f_{5/2} ($E_B = 393.5$ eV) and U4f_{7/2} ($E_B = 382.5$ eV), demonstrating the absence of redox reaction during the process of adsorption [38]. The SEM image of TAA–AC–U was shown in Fig. 3c. It was observed that the surface of TAA–AC became smoother after adsorption of U(VI). It indicated that a mass of tiny pores and indentations on the surface of TAA–AC provided plentiful active centers for adsorption reaction and which were filled up by uranium. The XRD spectra of the TAA–AC and TAA–AC–U were presented in Fig. S2. It showed that the broad peaks at 2θ of 24° and 43° corresponded to reflections of (002) and (100)

planes of amorphous carbon being graphitized slightly, and there were no significant changes in the chemical structure of TAA–AC after adsorption. The results indicated that the adsorbent was stable in acidic uranium solution. The FTIR spectrum of TAA–AC–U (Fig. 2a) showed that the peak of hydroxyl at 3142 cm^{-1} shifted to 3213 cm^{-1} ; the peak at 1398 cm^{-1} shifted to 1410 cm^{-1} and the peak of C=S group at 1120 cm^{-1} shifted to 1145 cm^{-1} . These results showed that the C=S, hydroxyl and amino groups of TAA–AC played a primary role in the adsorbent uranium interaction. The possible interaction mechanism between U(VI) and TAA–AC was shown in Fig. 5. In acid solution ($\text{pH} \leq 4$), U(VI) existed mainly in the form of UO_2^{2+} ions [13]. Two oxygen atoms of UO_2^{2+} ion coordinate with the uranium atom to form a central axis of linear structure, and the complexing ligands are located in the plane which is perpendicular to the central axis. The number of ligands is usually 4–6 [39–41]. The sulfur and oxygen atoms on TAA–AC would tend to chelate the uranyl ions to form hexatomic ring structure, in which the nitrogen can also coordinate with the uranium as an electron donor. Therefore, the uranyl ions can form a stable hexa-coordination chelate with the donor atoms in two rings.

Optimization of adsorption parameters

The effect of pH on the adsorption of U(VI) onto the TAA–AC over the range from 1.5 to 6 was shown in Fig. 6a. It could be seen that the adsorption rate increased as the pH increased from 1.5 to 2.0. At lower pH, the surface of the adsorbent would be closely associated with protons (H_3O^+) which could hinder the charged metal ions reaching the binding sites [42]. As pH increased from 2.0 to 3.5, uranium adsorption rate increased slowly from 92.1 to 98.2%, and the distribution coefficient grew obviously. It was found that the distribution coefficient was 2717 mL g^{-1} even at pH 1.5, which meant the TAA–AC possessed

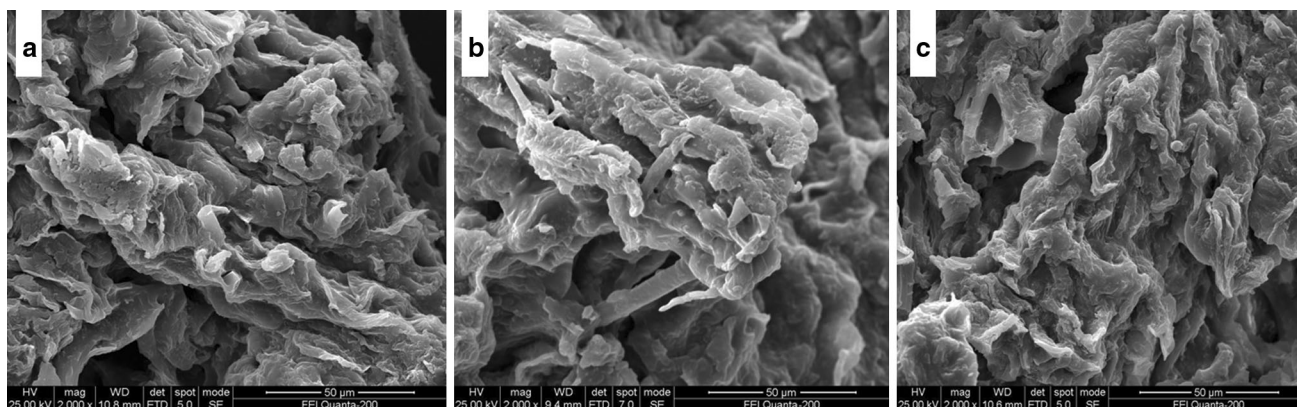


Fig. 3 SEM images of the surfaces of **a** AC, **b** TAA–AC, and **c** TAA–AC–U

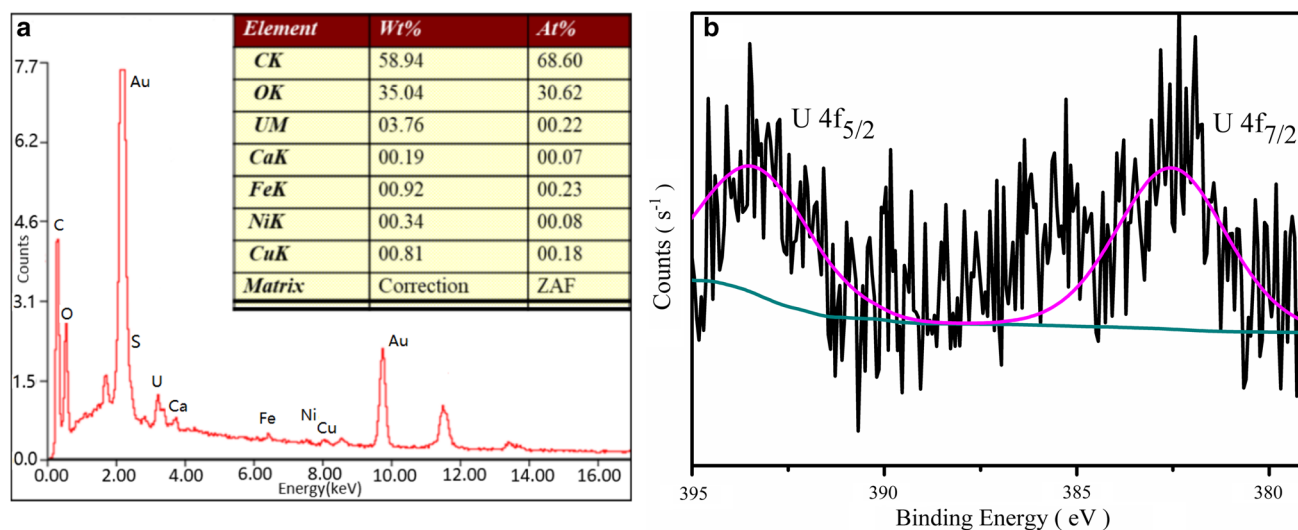
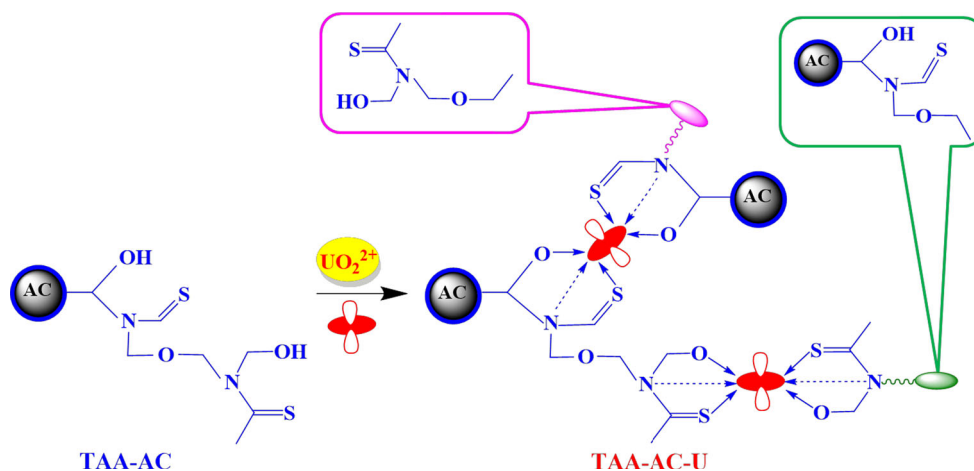


Fig. 4 **a** EDX spectra and **b** high-resolution U4f deconvoluted XPS spectra of TAA-AC-U

Fig. 5 Probable adsorption mechanism of U(VI) on TAA-AC



strong binding ability with uranium in acidic solution. When pH was 3.5, the adsorption rate reached the maximum. While pH increased to 4, the adsorption rate decreased slightly. When pH varied from 4 to 5, the adsorption rate kept almost unchanged. When pH value was higher than 5, the adsorption rate declined. The test was not conducted for pH higher than 6 due to the precipitation of uranium ions. The pH_{pzc} of TAA-AC was around 3.2 as presented in Fig. S3 (The measuring method was shown in Text S1), which was slightly lower than the optimal pH. This indicates that there were not only electrostatic force but also other promotion factor in the adsorption process. The possible reason was that the TAA-AC tended to bind with the linear ion of UO_2^{2+} which mainly existed below pH 4.

The effect of adsorption time on the adsorption of U(VI) onto the TAA-AC was shown in Fig. 6b. It can be seen that the adsorption process was divided into quick and slow

reaction stages within 2 h equilibrium time, and the whole speed of U(VI) adsorption onto the TAA-AC was satisfactory. The adsorption efficiency of U(VI) on TAA-AC increased to 92.3% rapidly in the first 20 min, and it then increased slowly until the equilibrium was reached in the following 2 h. Thereafter, the adsorption efficiency decreased slightly with the increasing of contact time, which was probably due to the minor desorption of uranium ions after adsorption balance.

The effect of temperature on the adsorption of U(VI) onto the TAA-AC was shown in Fig. 6c. It could be seen that the adsorption rate increased fast from 288 to 298 K. Subsequently, the adsorption rate increased slowly as the temperature increased from 298 to 308 K. The adsorption rate reached the maximum value of 98.1% at 308 K. The adsorption of uranium ions on the TAA-AC was mainly chemical one. Because physical adsorption was generally an exothermic process, the adsorption rate decreased when

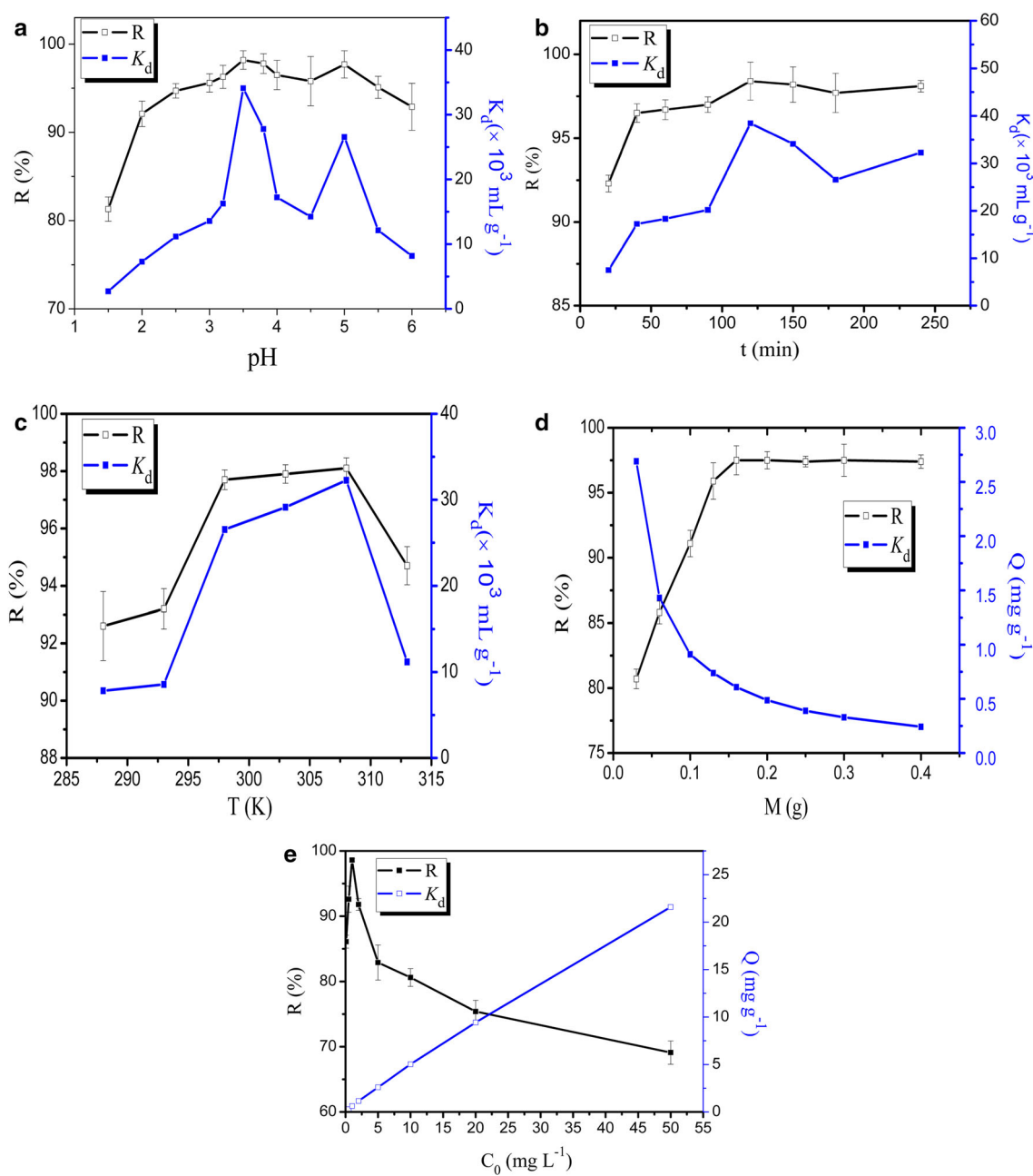


Fig. 6 Effects of **a** pH ($t = 120$ min, $C_0 = 1$ mg L⁻¹, $V = 100$ mL, $M = 0.16$ g, $T = 308$ K), **b** contact time (pH = 3.5, $C_0 = 1$ mg L⁻¹, $V = 100$ mL, $M = 0.16$ g, $T = 308$ K), **c** temperature (pH = 3.5, $t = 120$ min, $C_0 = 1$ mg L⁻¹, $V = 100$ mL, $M = 0.16$ g), **d** adsorbent

dose (pH = 3.5, $t = 120$ min, $C_0 = 1$ mg L⁻¹, $V = 100$ mL, $T = 308$ K), **e** initial concentration (pH = 3.5, $t = 120$ min, $V = 100$ mL, $M = 0.16$ g, $T = 308$ K) on the adsorption of U(VI) onto TAA-AC

the temperature increased. For chemical adsorption, the rise of temperature would increase the molecular collision and the adsorption reaction rate. When the temperature increased above 308 K, the adsorption rate decreased. The reason for this may be that the over high temperature hindered the adsorption of uranium ions on the TAA-AC and caused desorption, and there was also physical reaction in the adsorption process.

The effects of adsorbent dosage on the adsorption of U(VI) onto TAA-AC were showed in Fig. 6d. The adsorption rate of uranium increased from 80.7 to 97.5% with the increasing of the TAA-AC dosage due to the increasing of active sites, and the adsorption capacity of U(VI) onto TAA-AC decreased from 2.69 to 0.61 mg g⁻¹. When the adsorbent quantity reached 0.16 g, the

adsorption tended to saturation, and then the adsorption rate did not increase any more.

The effects of initial U(VI) concentration on the adsorption were investigated as shown in Fig. 6e. The result showed that the adsorption capacity of TAA–AC increased from 0.056 to 21.6 mg g⁻¹ when the initial U(VI) concentration increased from 0.1 to 50 mg L⁻¹. In general, the adsorption of uranium ions was more difficult from wastewater with low uranium concentration than that with high concentration, because the uranium ions in the wastewater with high concentration could provide great driving force surmounting the mass transfer resistance between solution and adsorbent, and the adsorption capacity of TAA–AC rose significantly with the initial uranium concentration.

Adsorption isotherms

Adsorption isotherms are fundamental in describing the distribution of the adsorbate in liquid and adsorbent. In order to obtain the maximum adsorption capacity of TAA–AC for U(VI), the adsorption isotherms were investigated at pH 3.5 with the initial U(VI) concentration ranging from 0.1 to 50 mg L⁻¹, respectively. The adsorption isotherms data were fitted by using Langmuir model, Freundlich model and Dubinin–Radushkevich model (the isotherm equations were shown in Text S1), respectively. The corresponding parameters of the three models were listed in Table 1, and the linear plots were shown in Fig. 7. It can be found that the isotherms data were fitted by Dubinin–Radushkevich model better than by Langmuir and Freundlich models, with the correlation coefficient (R^2) being over 0.98. The maximum adsorption capacities (Q_{\max}) of U(VI) on TAA–AC calculated by Langmuir model and Dubinin–Radushkevich model were as high as 30.21 and 340.34 mg g⁻¹, respectively. The adsorption isotherm at high uranium concentration was investigated (Fig. S4), and the results showed that the saturated adsorption capacity was 343 mg g⁻¹, which was consistent with the theoretical calculation. The maximum adsorption capacities of U(VI) on different adsorbents in acid solution were comparable as showed in Table 2, which revealed the potential application of TAA–AC in removal and recovery of U(VI)

from large amounts of acid aqueous solutions, especially from wastewater with low uranium concentration. The free energy value of E calculated from Dubinin–Radushkevich model was 10.4 kJ mol⁻¹, and it indicated that the sorption process was dominated by chemical adsorption [35].

Kinetic models

Adsorption kinetics was used to study the speed of adsorption, which was closely related to the contact time, and can provide valuable information for the adsorption mechanism. In view of this, the experimental kinetic data were simulated by pseudo first order model, pseudo second order model and intraparticle diffusion model (the equations of the kinetics models were shown in Text S3). The obtained kinetic parameters from the three models were listed in Table 3, and the plots of these models were shown in Fig. 8. The adsorption kinetic data for adsorption of U(VI) onto TAA–AC fitted the pseudo second order model better than the pseudo first order and the intraparticle diffusion models, with the correlation coefficient (R^2) being over 0.99, and besides, the calculated adsorption capacity $Q_{e,cal}$ was in good agreement with the experimental adsorption capacity $Q_{e,exp}$. These results suggested that the adsorbing speed was controlled by chemical adsorption rather than physical adsorption [51], and the adsorption behavior might involve electrostatic interaction and coordination bonding.

Thermodynamic studies

Figure 9 showed the plot of $\ln K_d$ versus $1/T$, and the thermodynamic parameters obtained from the plot were presented in Table 4 (The thermodynamic equation was shown in Text S4). The value of Gibbs free energy change (ΔG^0) was negative and decreased with increasing temperature, which showed that the adsorption of U(VI) ions was spontaneous and more favorable at higher temperature from 283 to 303 K. Low temperature would restrict the movement of molecules and decrease the rate of adsorption reaction. The positive value of enthalpy change (ΔH^0) indicated the endothermic nature in the adsorption process. The positive value of entropy change (ΔS^0) demonstrated

Table 1 Langmuir, Freundlich and Dubinin–Radushkevich equilibrium constants for adsorption of U(VI) onto TAA–AC

| Langmuir | | | | Freundlich | | | Dubinin–Radushkevich | | | | Experiment |
|-------------------------------------|------------------------------|-------|--------|------------|--------|--------|-------------------------------------|---|-----------------------------|--------|--------------------------------------|
| Q_{\max} (mg g ⁻¹) | b (L mg ⁻¹) | R_L | R^2 | K_f | n | R^2 | Q_{\max} (mg g ⁻¹) | β (mol ² J ⁻²) | E (kJ mol ⁻¹) | R^2 | $Q_{e,max}$ (mg g ⁻¹) |
| 30.21 | 0.131 | 0.202 | 0.8285 | 3.3925 | 1.3031 | 0.9512 | 340.34 | 4.59×10^{-9} | 10.4 | 0.9832 | 343 |

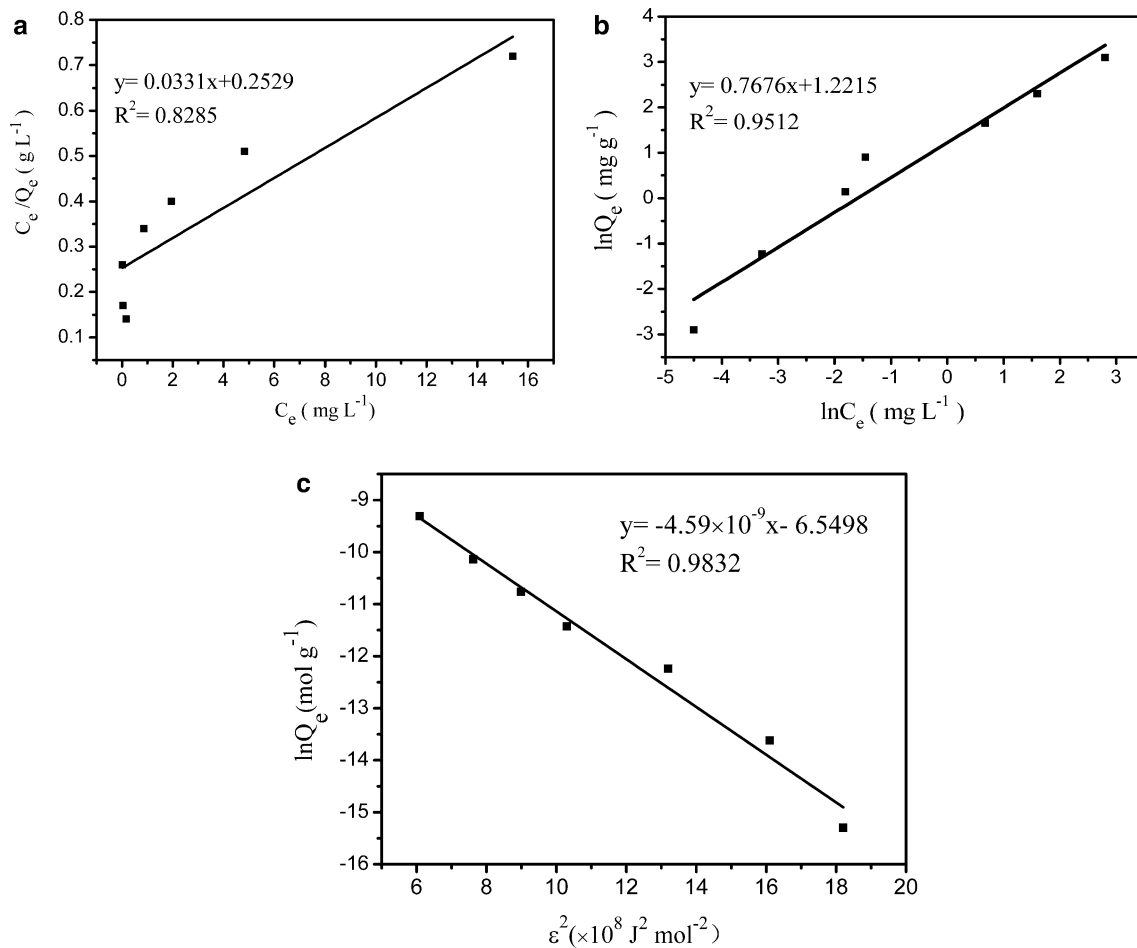


Fig. 7 Plots of **a** Langmuir, **b** Freundlich, and **c** Dubinin–Radushkevich models for adsorption of U(VI) onto TAA–AC

Table 2 Adsorption capacities of different adsorbents for U(VI) in acid solution

| Biosorbents | Q_{\max} (mg g ⁻¹) | pH | Initial concentration (mg L ⁻¹) | References |
|--|----------------------------------|-----|---|------------|
| <i>Vigna radiata</i> biomass | 294.1 | 4 | 50 | [43] |
| IRA-402 | 213 | 3 | 100 | [22] |
| Ambersep 920U SO4 | 62.5 | 2 | 250 | [44] |
| Activated carbon | 45.2 | 0 | 200 | [25] |
| Chitosan | 72.46 | 3 | 50 | [4] |
| TOA impregnated AC | 40.8 | 3.4 | 84 | [45] |
| Hydrothermal carbon | 347.9 | 4.5 | 100 | [46] |
| <i>Pleurotus ostreatus</i> | 19.44 | 4 | 10 | [47] |
| Polyethyleneimine modified AC | 115.3 | 5 | 10 | [48] |
| Nano-Fe ₃ O ₄ -urea-AC | 46.65 | 5 | 30 | [49] |
| BT-AC | 82 | 4.5 | 100 | [50] |
| TAA-AC | 340.34 | 3.5 | 1 | This work |

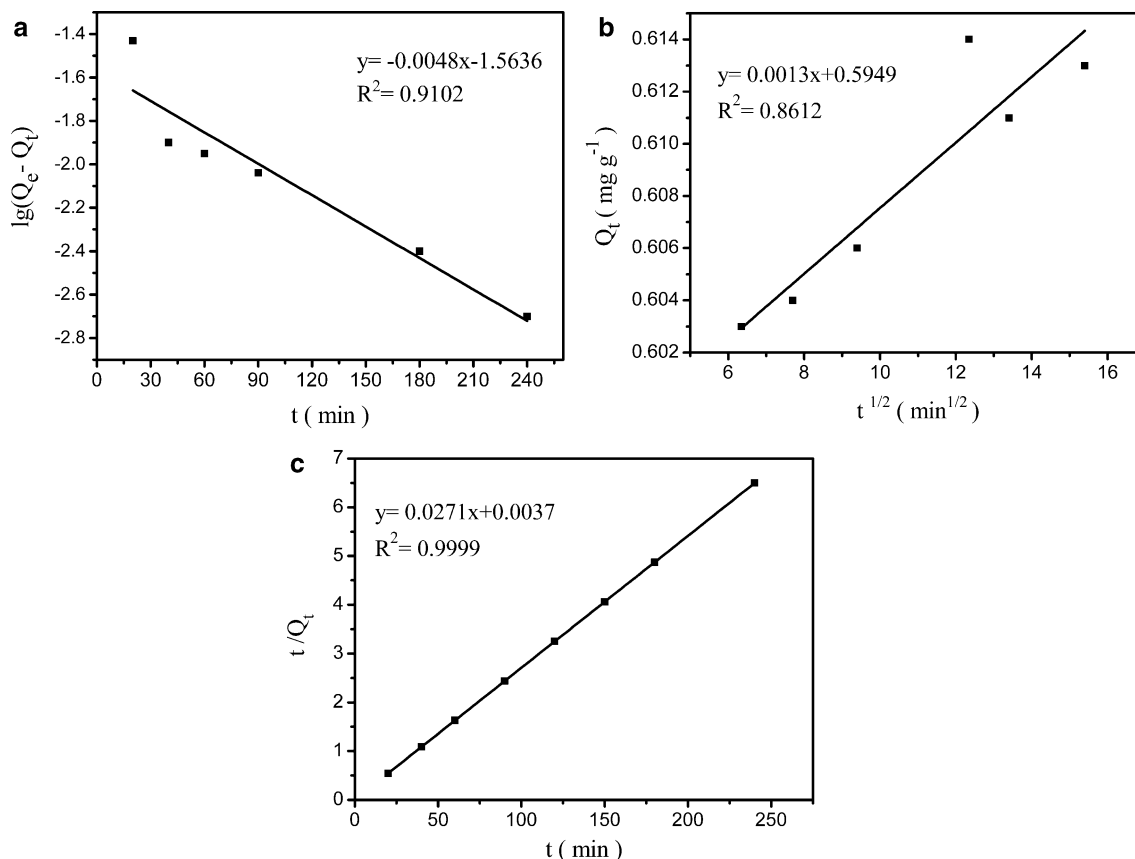
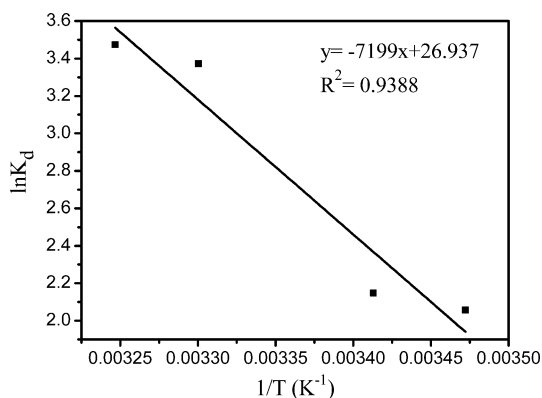
the randomness at the solid/solution interface would increase during the adsorption process, which was due to the desorption of the water molecular [35, 52], and it also indicated strong affinity and spontaneity of the adsorption process.

Selective adsorption

The selective adsorption of U(VI) onto TAA-AC was studied using the simulated water sample containing Ca(II), Mg(II), Zn(II), Fe(III), Ni(II), Mn(II), Hg(II), Se(IV) and

Table 3 Kinetic parameters for adsorption of U(VI) onto TAA–AC

| Pseudo first order | | | Pseudo second order | | | Intraparticle diffusion | | |
|-----------------------------|-----------------------------|--------|-----------------------------|---|--------|--|----------------------------|--------|
| Q_e (mg g ⁻¹) | K_1 (L mg ⁻¹) | R^2 | Q_e (mg g ⁻¹) | K_2 (mg g ⁻¹ min ⁻¹) | R^2 | K_{id} (mg g ⁻¹ min ^{-0.5}) | C (mol J ⁻²) | R^2 |
| 0.027 | 0.011 | 0.9076 | 36.9 | 0.198 | 0.9999 | 0.0013 | 0.595 | 0.8612 |

**Fig. 8** Plots of **a** pseudo first order, **b** intraparticle diffusion, and **c** pseudo second order models for adsorption of U(VI) onto TAA–AC**Fig. 9** Liner plot of $\ln K_d$ against $1/T$ for adsorption of U(VI) onto TAA–AC

U(VI). The initial metal ion concentrations were 1 mg L⁻¹. The concentrations of residual Ca(II), Mg(II), Zn(II), Fe(III), Ni(II), Mn(II) were detected by TAS-990A atomic absorption spectrophotometer, and the concentrations of Hg(II) and Se(IV) were detected by AFS-8220 atomic fluorescent spectrometer. The selectivity coefficient ($S_{U(VI)/M}$) for U(VI) ions with respect to the competitive ions were calculated using the following equation [34]:

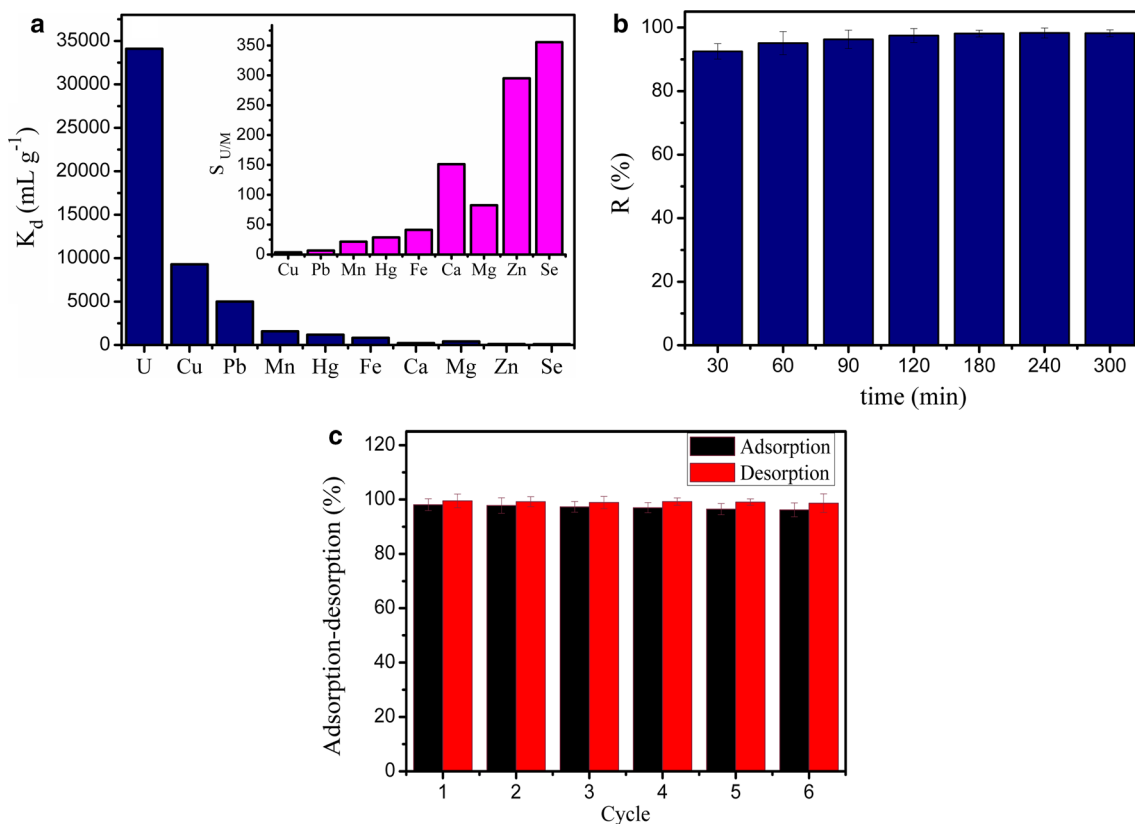
$$S_{U(VI)/M} = \frac{K_{d(U)}}{K_{d(M)}} \quad (4)$$

where $K_{d(U)}$ and $K_{d(M)}$ were distribution coefficients of TAA–AC for U(VI) and other competitive ions, respectively.

As shown in Fig. 10a, the K_d values of other metal ions were lower than that of U(VI), and $S_{U(VI)/M}$ values of other

Table 4 Thermodynamic parameters for adsorption of U(VI) onto TAA-AC

| ΔH^0 (kJ mol ⁻¹) | ΔS^0 (J mol ⁻¹ K ⁻¹) | ΔG^0 (kJ mol ⁻¹) | | | |
|--------------------------------------|---|--------------------------------------|---------|---------|---------|
| | | 288 K | 293 K | 303 K | 308 K |
| 59.85 | 223.87 | - 4.925 | - 5.232 | - 8.495 | - 8.896 |

**Fig. 10** **a** Effects of competitive ions on the selective adsorption of U(VI) (pH = 3.5, $C_0 = 1 \text{ mg L}^{-1}$ for all cations, $T = 308 \text{ K}$, $t = 4 \text{ h}$, $V = 100 \text{ mL}$, $M = 0.16 \text{ g}$), **b** adsorption rate of U(VI) from actualacid wastewater ($V = 100 \text{ mL}$, $T = 308 \text{ K}$, $M = 0.16 \text{ g}$), **c** six cycles of adsorption–desorption of U(VI) by TAA-AC

metal ions were higher than that of U(VI). It was found that Ca(II), Mg(II), Zn(II), Fe(III), Ni(II), Mn(II), Hg(II) and Se(IV) had no obvious interference with the adsorption of U(VI) onto TAA-AC, and TAA-AC had good selectivity for U(VI) ions in solution containing other metal ions. The possible reason for high selectivity for U(VI) ions was that UO_2^{2+} had a linear structure ($\text{O}=\text{U}=\text{O}$), which could form more stable hexa-coordination by chelating with electron donors (sulfur, oxygen and nitrogen atoms) on the surface of TAA-AC.

Treatment of actual radioactive wastewater with low uranium concentration

Based on the above experimental results, the TAA-AC was further applied to the treatment of actual acid wastewater

with low uranium concentration from an in situ leach uranium mine ($C_{\text{U(VI)}} = 1.047 \text{ mg L}^{-1}$). The wastewater contained a vast amount of cations and anion ions (The composition of the wastewater was shown in Table S2), and some of them had the concentrations which are hundreds times as high as that of U(VI). As shown in Fig. 10b, U(VI) was still effectively adsorbed onto TAA-AC not only from synthetic wastewater but also from the actual acid wastewater. The adsorption rate increased with the increasing adsorption time, the major adsorption of U(VI) was accomplished in the first 30 min, the adsorption equilibrium was reached within 180 min. The removal efficiency and the distribution coefficient (K_d) for U(VI) were 98.3% and $3.78 \times 10^4 \text{ mL g}^{-1}$, respectively. The results showed that TAA-AC could effectively remove uranium from the actual wastewater without pH

adjustment, and it was a promising adsorbent for treating the actual wastewater with low uranium concentration.

Regeneration and reusability

The regeneration-reuse property is important for the application of adsorbents in real work, because an appropriate adsorbent should present not only excellent selective adsorption capability but also regeneration-reuse property. In the present study, the reusability of TAA-AC was investigated by washing with different desorption agent and rinsing with ultrapure water thoroughly. As can be seen from Fig. 10c, 0.5 mol L⁻¹ HNO₃ was the best eluant for the desorption, the desorption efficiency was above 98%, and the regenerated TAA-AC showed the similar removal rate of U(VI) as the fresh TAA-AC. It was found that the TAA-AC loaded with U(VI) could easily be regenerated with ordinary acidic solution, and the mechanism of desorption was mainly ascribed to the ion-exchange between the aqueous H⁺ and UO₂²⁺ on the adsorbent. Moreover, there was only a slight decrease (from 98.1 to 96.2%) in the adsorption rate after six cycles of regeneration-reuse (Fig. 10c). The results indicated that the TAA-AC could easily be reused for adsorbing U(VI) from radioactive wastewater, and it would have good prospects in practical applications.

Conclusion

In this study, a novel material TAA-AC was prepared from liquorice residue as an adsorbent for removal and recovery of U(VI) from acid wastewater with low uranium concentration. The effects of the initial pH, contact time, temperature, adsorbent dose and initial U(VI) concentration on the adsorption behavior by TAA-AC were investigated. The results showed that TAA-AC had high removal rate for U(VI) in the solution of 1 mg L⁻¹ uranium at pH 2–6. The adsorption data were best fitted by the Dubinin–Radushkevich isotherm model, and the maximum adsorption capacity of TAA-AC for U(VI) was 340 mg g⁻¹. The adsorption kinetics was in good agreement with the pseudo-second order model. The Gibbs free energy change (ΔG^0), enthalpy change (ΔH^0) and entropy change (ΔS^0) showed that the adsorption process of U(VI) was spontaneous, feasible and endothermic. In the presence of competitive ions such as Ca(II), Mg(II), Zn(II), Fe(III), Ni(II), Mn(II), Hg(II) and Se(IV), TAA-AC showed an enhanced selectivity for uranium due to the stable hexacoordination formed by UO₂²⁺ chelating with electron donors. The high adsorption rate (98.3%) and selectivity ($K_d = 3.78 \times 10^4$ mL g⁻¹) were observed in actual acid

mine wastewater. The desorption efficiency was above 98%, and the adsorbent rate maintained 96.2% over six cycles. This work provided a cost effective and selective adsorbent for adsorption and recovery of U(VI) from the actual acid radioactive wastewater with low uranium concentration from the in situ leach uranium mine.

Acknowledgements This research was supported by the National Natural Science Foundation of China (U1401231, 11405081 and 51704170), the Development Program for Science and Technology for National Defense (B3720132001), the China Postdoctoral Science Foundation (2017M612569), and the Research Foundation of Education Bureau of Hunan Province (16C1386).

References

1. Wang X, Wang T, Zheng X, Shen Y, Lu X (2017) Isotherms, thermodynamic and mechanism studies of removal of low concentration uranium(VI) by *Aspergillus niger*. *Water Sci Technol* 75(12):2727–2736
2. Abdi S, Nasiri M, Mesbahi A, Khani MH (2017) Investigation of uranium(VI) adsorption by polypyrrole. *J Hazard Mater* 332:132–139
3. Bayramoglu G, Celik G, Arica MY (2006) Studies on accumulation of uranium by fungus *Lentinus sajor-caju*. *J Hazard Mater* 136(2):345–353
4. Wang G, Liu J, Wang X, Xie Z, Deng N (2009) Adsorption of uranium(VI) from aqueous solution onto cross-linked chitosan. *J Hazard Mater* 168(2–3):1053–1058
5. Favas PJ, Pratas J, Mitra S, Sarkar SK, Venkatachalam P (2016) Biogeochemistry of uranium in the soil-plant and water-plant systems in an old uranium mine. *Sci Total Environ* 568:350–368
6. Chen C, Wang J (2016) Uranium removal by novel graphene oxide-immobilized *Saccharomyces cerevisiae* gel beads. *J Environ Radioact* 162–163:134–145
7. Kong L, Su M, Mai Z, Li H, Diao Z, Xiong Y, Chen D (2017) Removal of uranium from aqueous solution by two-dimensional electrosorption reactor. *Environ Technol Innov* 8:57–63
8. Li C, Wei Y, Wang X, Yin X (2018) Efficient and rapid adsorption of iodide ion from aqueous solution by porous silica spheres loaded with calcined Mg–Al layered double hydroxide. *J Taiwan Inst Chem Eng* 85:193–200
9. Paschalidou P, Liatsou I, Pashalidis I, Theocharis CR (2017) Effect of surface and textural characteristics on uranium adsorption by nanoporous titania. *J Radioanal Nucl Chem* 314(2):1141–1147
10. Ghasemi Torkabad M, Keshtkar AR, Safdari SJ (2017) Comparison of polyethersulfone and polyamide nanofiltration membranes for uranium removal from aqueous solution. *Prog Nucl Energy* 94:93–100
11. Chen L, Chen Y, Wang X, Wei Y, He L, Tang F (2017) A novel silica-based anion exchange resin used for removing uranium from drinking water. *J Radioanal Nucl Chem* 314(3):2569–2578
12. Yu J, Wang J, Jiang Y (2017) Removal of uranium from aqueous solution by alginate beads. *Nucl Eng Technol* 49(3):534–540
13. Nekhunguni PM, Tavengwa NT, Tutu H (2017) Sorption of uranium(VI) onto hydrous ferric oxide-modified zeolite: assessment of the effect of pH, contact time, temperature, selected cations and anions on sorbent interactions. *J Environ Manag* 204(Pt 1):571–582
14. Dangelmayr MA, Reimus PW, Wasserman NL, Punsal JJ, Johnson RH, Clay JT, Stone JJ (2017) Laboratory column

- experiments and transport modeling to evaluate retardation of uranium in an aquifer downgradient of a uranium in situ recovery site. *Appl Geochem* 80:1–13
15. Wang F, Liu Q, Li R, Li Z, Zhang H, Liu L, Wang J (2016) Selective adsorption of uranium(VI) onto prismatic sulfides from aqueous solution. *Colloids Surf A* 490:215–221
 16. Gao X, Bi M, Shi K, Chai Z, Wu W (2017) Sorption characteristic of uranium(VI) ion onto K-feldspar. *Appl Radiat Isot* 128:311–317
 17. Anirudhan TS, Nima J, Divya PL (2015) Adsorption and separation behavior of uranium(VI) by 4-vinylpyridine-grafted-vinyltriethoxysilane-cellulose ion imprinted polymer. *J Environ Chem Eng* 3(2):1267–1276
 18. Bhargava SK, Ram R, Pownceby M, Grocott S, Ring B, Tardio J, Jones L (2015) A review of acid leaching of uraninite. *Hydrometallurgy* 151:10–24
 19. Miśkiewicz A, Zakrzewska-Kołtuniewicz G, Dłuska E, Walo PF (2016) Application of membrane contactor with helical flow for processing uranium ores. *Hydrometallurgy* 163:108–114
 20. Douglas G, Shackleton M, Woods P (2014) Hydrotalcite formation facilitates effective contaminant and radionuclide removal from acidic uranium mine barren lixiviant. *Appl Geochem* 42:27–37
 21. Perdrial N, Vázquez-Ortega A, Wang G, Kanematsu M, Mueller KT, Um W, Steefel CI, O'Day PA, Chorover J (2018) Uranium speciation in acid waste-weathered sediments: the role of aging and phosphate amendments. *Appl Geochem* 89:109–120
 22. Solgy M, Taghizadeh M, Ghoddocynejad D (2015) Adsorption of uranium(VI) from sulphate solutions using Amberlite IRA-402 resin: equilibrium, kinetics and thermodynamics study. *Ann Nucl Energy* 75:132–138
 23. Ölmez Ş, Eral M (1994) Extraction of uranium from acidic solutions by TBP impregnated polyurethane foam. In: Kučera J, Obrusník I, Sabbioni E (eds) *Nuclear analytical methods in the life sciences*. Humana Press, Totowa, pp 731–735
 24. Hussein AEM, Taha MH (2012) Uranium removal from nitric acid raffinate solution by solvent immobilized PVC cement. *J Radioanal Nucl Chem* 295(1):709–715
 25. Morsy AMA, Hussein AEM (2011) Adsorption of uranium from crude phosphoric acid using activated carbon. *J Radioanal Nucl Chem* 288(2):341–346
 26. Oyewo OA, Onyango MS, Wolkersdorfer C (2016) Application of banana peels nanosorbent for the removal of radioactive minerals from real mine water. *J Environ Radioact* 164:369–376
 27. Zhang G, Qu J, Liu H, Cooper AT, Wu R (2007) CuFe_2O_4 /activated carbon composite: a novel magnetic adsorbent for the removal of acid orange II and catalytic regeneration. *Chemosphere* 68(6):1058–1066
 28. Abbasi A, Streat M (1998) Sorption of uranium from nitric acid solution using Tbp-impregnated activated carbons. *Solvent Extr Ion Exchange* 16(5):1303–1320
 29. Enniya I, Rghioui L, Jourani A (2018) Adsorption of hexavalent chromium in aqueous solution on activated carbon prepared from apple peels. *Sustain Chem Pharm* 7:9–16
 30. Hong S, Cannon FS, Hou P, Byrne T, Nieto-Delgado C (2017) Adsorptive removal of sulfate from acid mine drainage by polypyrrole modified activated carbons: effects of polypyrrole deposition protocols and activated carbon source. *Chemosphere* 184:429–437
 31. Chen S, Hong J, Yang H, Yang J (2013) Adsorption of uranium (VI) from aqueous solution using a novel graphene oxide-activated carbon felt composite. *J Environ Radioact* 126:253–258
 32. Al-Malack MH, Dauda M (2017) Competitive adsorption of cadmium and phenol on activated carbon produced from municipal sludge. *J Environ Chem Eng* 5(3):2718–2729
 33. Kaghazchi T, Kolar NA, Soleimani M (2010) Licorice residue and Pistachio-nut shell mixture: a promising precursor for activated carbon. *J Ind Eng Chem* 16(3):368–374
 34. Kaghazchi T, Soleimani M, Yeganeh MM (2006) Production of activated carbon from residue of liquorices chemical activation. In: 8th Asia-Pacific international symposium on combustion and energy utilization, Sochi, Russian. ISBN 5-89238-086-6
 35. Ding DX, Xin X, Li L, Hu N, Li GY, Wang YD, Fu PK (2014) Removal and recovery of U(VI) from low concentration radioactive wastewater by ethylenediamine-modified biomass of *Aspergillus niger*. *Water Air Soil Pollut* 225(12):2206
 36. Li L, Hu N, Ding D, Xin X, Wang Y, Xue J, Zhang H, Tan Y (2015) Adsorption and recovery of U(VI) from low concentration uranium solution by amidoxime modified *Aspergillus niger*. *RSC Adv* 5(81):65827–65839
 37. Jaouadi M, Hbaieb S, Guedidi H, Reinert L, Amdouni N, Duclaux L (2017) Preparation and characterization of carbons from β -cyclodextrin dehydration and from olive pomace activation and their application for boron adsorption. *J Saudi Chem Soc* 21(7):822–829
 38. Husnain SM, Kim HJ, Um W, Chang YY, Chang YS (2017) Superparamagnetic adsorbent based on phosphonate grafted mesoporous carbon for uranium removal. *Ind Eng Chem Res* 56(35):9821–9830
 39. Si ZX, Xu W, Zheng YQ (2016) Synthesis, structure, luminescence and photocatalytic properties of an uranyl-2, 5-pyridinedicarboxylate coordination polymer. *J Solid State Chem* 239:139–144
 40. Sessler JL, Seidel D, Vivian AE, Lynch V, Scott BL, Keogh DW (2001) Hexaphyrin (1.0. 1.0. 0.0): an expanded porphyrin ligand for the actinide cations uranyl (UO_2^{2+}) and neptunyl (NpO_2^+). *Angew Chem Int Ed* 40(3):591–594
 41. Unruh DK, Libo A, Streicher L, Forbes TZ (2014) Synthesis and characterization of 1-D uranyl thiodiglycolate coordination polymers. *Polyhedron* 73:110–117
 42. Mezaguer M, Neh K, Lounici H, Kamel Z (2012) Characterization and properties of *Pleurotus mutilus* fungal biomass as adsorbent of the removal of uranium(VI) from uranium leachate. *J Radioanal Nucl Chem* 295(1):393–403
 43. Naeem H, Bhatti HN, Sadaf S, Iqbal M (2017) Uranium remediation using modified *Vigna radiata* waste biomass. *Appl Radiat Isot* 123:94–101
 44. Cheira MF, Atia BM, Kouraim MN (2017) Uranium(VI) recovery from acidic leach liquor by Ambersep 920U SO 4 resin: kinetic, equilibrium and thermodynamic studies. *J Radiat Res Appl Sci* 10(4):307–319
 45. Ahmed SH, Sharaby CM, El Gammal EM (2013) Uranium extraction from sulfuric acid medium using triocetylamine impregnated activated carbon. *Hydrometallurgy* 134–135:150–157
 46. Li B, Ma L, Tian Y, Yang X, Li J, Bai C, Yang X, Zhang S, Li S, Jin Y (2014) A catechol-like phenolic ligand-functionalized hydrothermal carbon: one-pot synthesis, characterization and sorption behavior toward uranium. *J Hazard Mater* 271:41–49
 47. Zhao C, Liu J, Tu H, Li F, Li X, Yang J, Liao J, Yang Y, Liu N, Sun Q (2016) Characteristics of uranium biosorption from aqueous solutions on fungus *Pleurotus ostreatus*. *Environ Sci Pollut Res Int* 23(24):24846–24856
 48. Saleh TA, Tuzen M, Sari A (2017) Polyethylenimine modified activated carbon as novel magnetic adsorbent for the removal of uranium from aqueous solution. *Chem Eng Res Des* 117:218–227
 49. Mahmoud ME, Khalifa MA, El Wakeel YM, Header MS, Abdel-Fattah TM (2017) Engineered nano-magnetic iron oxide-urea-

- activated carbon nanolayer sorbent for potential removal of uranium(VI) from aqueous solution. *J Nucl Mater* 487:13–22
50. Zhao Y, Liu C, Feng M, Chen Z, Li S, Tian G, Li S (2010) Solid phase extraction of uranium(VI) onto benzoylthiourea-anchored activated carbon. *J Hazard Mater* 176(1–3):119–124
51. Liu Y, Dai Y, Yuan D, Wang Y, Zou L (2017) The preparation of PZS-OH/CNT composite and its adsorption of U(VI) in aqueous solutions. *J Radioanal Nucl Chem* 314(3):1747–1757
52. Bulut Y, Tez Z (2007) Removal of heavy metals from aqueous solution by sawdust adsorption. *J Environ Sci* 19(2):160–166